ELSEVIER

Journal of Organometallic Chemistry 507 (1996) 85–101

Journal of Organometallic Chemistry

Palladium(II) complexes of chiral tridentate nitrogen pybox ligands

Reinhard Nesper [a], Paul Pregosin [a,*], Kurt Püntener [a], Michael Wörle [a], Alberto Albinati [b]

[a] *Inorganic Chemistry, ETH-Zentrum, CH-8092 Zürich, Switzerland*
[b] *Chemical Pharmacy, University of Milan, I-20131 Milan, Italy*

Received 1 March 1995; in revised form 16 May 1995

Abstract

A series of mono- and di-cationic palladium(II) complexes containing different chiral tridentate nitrogen ligands, pybox, have been prepared [pybox = 2,6-bis[4′-(*S*)-^{i}Pr (or Ph, or Bz or *p*-EtOC_6H_4)oxazoline-2′-yl]pyridine (**1–4**), respectively]. The molecular structures for two of these, $[Pd(CH_3CN)(\mathbf{2})](BF_4)_2$ (**6**) and $[Pd(PPh_3)(\mathbf{3})](BF_4)_2$ (**21g**), have been determined by X-ray diffraction and show no major steric hindrance in the fourth coordination position. In connection with the aldol reaction of $CNCH_2CO_2Me$ with PhCHO, several new isonitrile Pd^{II} complexes have also been prepared. It is shown that, under catalytic conditions, the chiral tridentate pybox ligand is completely displaced, thus explaining its failure as a chiral auxiliary. Preparative details for a series of chiral $Pd(L)(\mathbf{3})^{n+}(BF_4)_n$ (**21**) complexes [L = 4-methylpyridine, 2,6-dimethylpyridine, 4-methyl aniline, $H_2NCH_2CH(OMe)_2$, $H_2NCH_2CH_2OH$, $H_2N(CH_2)_5CH_3$, N_3^-, HCO_2^-, Cl^-] are given, as are preparative details for some model Pd^{II} acetonitrile complexes with chiral phosphorus and nitrogen chelating ligands. For **6**, i.e. $PdC_{25}H_{22}N_4O_2B_2F_8$, the crystals are monoclinic with space group $P2_1$ (No. 4), $a = 13.582(6)$ Å, $b = 13.826(6)$ Å, $c = 14.667(6)$ Å, $\beta = 97.28(3)°$, $V = 2732(2)$ Å^3, $Z = 4$. For **21g**, i.e. $C_{43}H_{38}B_2F_8N_3O_2P_2Pd$, the crystals are orthorhombic with space group, $P2_12_12_1$, $a = 10.616(4)$ Å, $b = 16.774(2)$ Å, $c = 23.086(4)$ Å, $V = 4111(3)$ Å^3, $Z = 4$.

Keywords: Palladium; Pybox; Isonitrile; Aldol condensation; X-Ray structure determination; NMR spectroscopy; IR spectroscopy; Mass spectrometry

1. Introduction

The organic chemistry of palladium continues to develop as an important synthetic tool [1]. The application of chiral Pd^{II} complexes as catalysts can afford organic products with substantial enantiomeric excesses [2], e.g., salts of Pd^{II} can be used [3] to catalyse reaction (1). Previously [4,5], salts of Au^I and Ag^I had been used for this reaction, with the former metal most frequently employed.

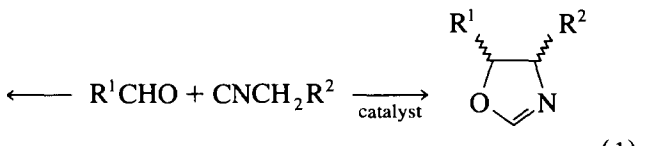

(1)

Several palladium complexes containing the chiral tridentate nitrogen ligand {(*S,S*-pybox)(^{i}Pr)}, in which (*S,S*)-pybox(^{i}Pr) = 2,6-bis[4′-(*S*)-isopropyloxazoline-2-yl]pyridine (**1**) have been tested. Unfortunately, the observed [3] enantiomeric excesses in the presence of this chiral nitrogen chelate were very modest, < 20%. We report here the synthesis and characterisation of new mono- and di-cationic pybox Pd^{II} complexes, with two of the latter having been characterised in the solid state via X-ray diffraction. Further, we offer an explanation for the failure of **1–4** with respect to potential chiral induction.

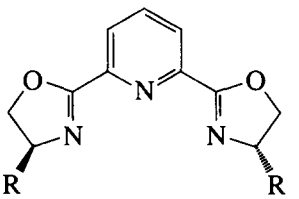

R = ^{i}Pr (**1**)
R = Ph (**2**)
R = CH_2Ph=Bz (**3**)
R = *p*-EtO—C_6H_4(*R,R*) (**4**)

* Corresponding author.

SSDI 0022-328X(95)05759-5

2. Results and discussion

2.1. Ligand preparation

The ligands were prepared as shown in Scheme 1 via the condensation of 0.5 equiv. of the commercially available 2,6-dicarbonyl chloride with 1 equiv. of the corresponding chiral amino alcohol (available or accessible from the *S*-amino acid).

The reaction proceeds through steps involving amide intermediates and in several runs we did not isolate the desired products but rather materials stemming from only one ring closure. Ligands 1–3 have been reported previously [3,6]. Ligand **4** was identified via microanalytical, FAB mass spectroscopic and NMR data and showed the expected C_2 symmetry. Analytical and other details are provided under Experimental details.

2.2. Acetonitrile complexes

The complexes $[Pd(CH_3CN)(pybox)](BF_4)_2$ **(5–8)** were prepared by addition of the tridentate ligand to the

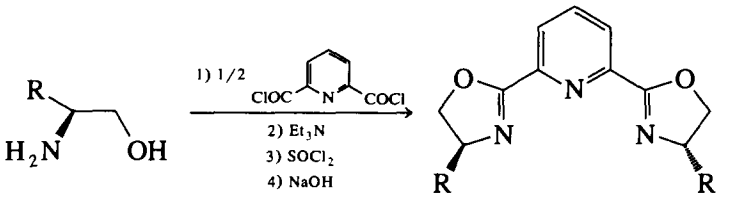

R = ^{i}Pr (**1**)
R = Ph (**2**)
R = Bz (**3**)
R = *p*-$EtOC_6H_4$ (**4**)

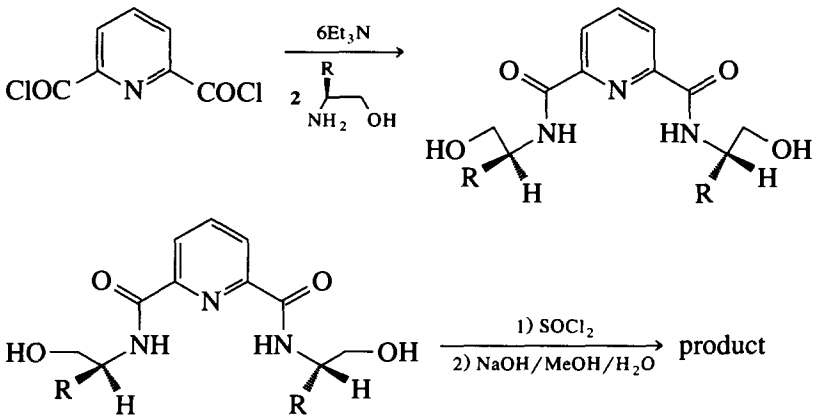

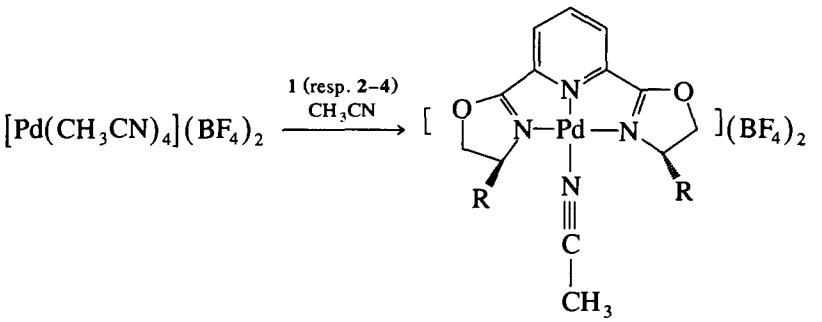

(5–8)

R = ^{i}Pr (**5**)
R = Ph (**6**)
R = Bz (**7**)
R = *p*-$EtOC_6H_4$ (**8**)

Scheme 1. Synthetic Pybox Chemistry

well-known tetrakis-acetonitrile complex $[Pd(CH_3CN)_4](BF_4)_2$ [7]. Compounds **5–8** were characterised via elemental analysis plus mass spectral, IR, NMR and conductivity measurements.

The solid-state structure for the phenyl derivative **6** was determined by X-ray diffraction. Details of the data collection are given in Table 1, positional parameters in Table 2, a list of selected bond lengths and bond angles in Table 3 and an ORTEP view of the dication in Fig. 1. The immediate coordination sphere is distorted square planar, with the major distortion arising via the N(11)–Pd(1)–N(13) angle, at 159.7(3)°. This angle is considerably smaller than the ideal angle of 180°, but consistent with *trans*-nitrogen donors held together by two fused five-membered rings [8]. As in the structure [3] of the ^{i}Pr analogue **5**, where this angle is 161.2(4)°, this *trans* arrangement is important in that it opens the front of the molecule, thus creating space for incoming ligands. In **6**, the angle N(12)–Pd(1)–N(14), involving the acetonitrile and the pyridine nitrogen, is normal at 176.3(5)°. The various Pd–N bond lengths are all consistent with nitrogen coordination; however, the Pd–N(12) length to the pyridine, 1.927(7) Å, is quite short [1.922(9) Å in **5**] and even shorter than the Pd–N(14) separation to acetonitrile, i.e. 1.968(9) Å. Surprisingly, the Pd–N(acetonitrile) in **6**, 1.968(9) Å, is slightly shorter than for **5**, 2.028(9) Å. In the model cation $Pd(CH_3CN)_2(bipy)]^{2+}$ [3], the Pd–N(nitrile) separation is 2.004(8) Å and the Pd–N(bipy) bond length is 1.992(7) Å. For the hydride complex *trans*-$[PdH(CH_3CN)(P^tBu_3)_2](BPh_4)$ [9], the Pd–N(nitrile) bond length is longer, 2.122(4) Å, in keeping with the difference in trans influence between a hydride and an sp^2-nitrogen donor [10]. The nitrile C–N distance in **6**, 1.163(14) Å, is as expected.

Interestingly, the structure of **6 clearly** shows that the phenyl rings are twisted so as to be almost perpendicu-

Table 1
Experimental data for the X-ray diffraction study of **[6]**$(BF_4)_2$ and **[21g]**$(BF_4)_2$

Compound	**[6]**$(BF_4)_2$	**[21g]**$(BF_4)_2$
Formula	$C_{25}H_{22}B_2F_8N_4O_2Pd$	$C_{43}H_{38}B_2F_8N_3O_2P_2Pd$
Mol. wt.	690.48	970.76
Crystal dimensions (mm)	0.38 × 0.34 × 0.53	0.10 × 0.20 × 0.25
Data collection temperature (°C)	23	23
Diffractometer	STOE scanner IPDS	CAD4
Cryst system	monoclinic	orthorhombic
Space group	$P2_1$	$P2_12_12_1$
a (Å)	13.582(6)	10.616(4)
b (Å)	13.826(6)	16.774(2)
c (Å)	14.667(6)	23.086(4)
β (°)	97.28(3)	
V (Å^3)	2732(2)	4111(3)
Z	4	4
ρ (calc.) (g cm^{-3})	1.679	1.568
μ (cm^{-1})	7.20	5.97
Radiation	Mo K α (graphite monochromated λ = 0.71069 Å)	
Measured reflections		$+h, +k, +l$
θ range (°)	$3.5 < \theta < 24.2$	$2.5 < \theta < 25.0$
Scan type		$\omega/2\theta$
Scan width (°)		1.10 + 0.35 tan θ
Maximum counting time (s)		100
Bkgd. time (s)		0.5 × scan-time
Prescan rejection limit		$0.50(2.00\sigma)$
Prescan acceptance limit		$0.025(40.0\sigma)$
No. data collected	15037	7290
No. independent data	7728	6870
No. observed reflections (n_o)	7104	3731
	$[\lvert F_o\rvert^2 > 5.0\sigma(\lvert F\rvert^2)]$	$[\lvert F_o\rvert^2 > 3.0\sigma(\lvert F\rvert^2)]$
Transmission coeff.		0.9269–0.9967
No. of parameters refined (n_v)	738	291
Fudge factor $f(k)$ [a,b]	0.0054 (1.00)	0.070
Maximum parameter shift $\Delta p/\sigma$ (at convergence)	< 0.2	< 0.1
R_{av} [a]	0.032	
R [a]	0.060	0.052
R_w [a]	0.070	0.062
GOF [a]	1.329	1.515

[a] $R_{av} = \Sigma_i \lvert F_{o,av} - F_{o,i}\rvert / \Sigma_i \lvert F_{o,av}\rvert$; $R = \Sigma \lvert\lvert F_o\rvert - 1/k\lvert F_c\rvert\rvert / \Sigma \lvert F_o\rvert$; $R_w = [\Sigma w(\lvert F_o\rvert - 1/k\lvert F_c\rvert)^2 / \Sigma w \lvert F_o\rvert^2]^{1/2}$ where $w = [\sigma^2(F_o)]^{-1}$ and $\sigma(F_o) = [\sigma^2(F_o^2) + f^2(F_o^2)^2]^{1/2}/2F_o$; [b] $w = k[\sigma^2(F_o) + \lvert f\rvert(F_o)^2]$; GOF = $[\Sigma w(\lvert F_o\rvert - (1/k)\lvert F_c\rvert)^2/(n_o - n_v)]^{1/2}$.

Table 2
Positional parameters and isotropic equivalent displacement parameters (pm^2) for $[\mathbf{6}](BF_4)_2$ (Complex **1**) with esds in parentheses

Atom	x	y	z	$U_{iso/equiv}$	Occupancy factor
Pd(1)	0.7463(1)	0.4687	1.0287(1)	340(10)	1
N(11)	0.7687(6)	0.3252(6)	1.0101(5)	370(20)	1
N(12)	0.7495(5)	0.4637(10)	0.8978(4)	360(20)	1
N(13)	0.7250(5)	0.6079(6)	0.9992(6)	390(30)	1
N(14)	0.7360(6)	0.4676(10)	1.1612(6)	490(30)	1
C(141)	0.7167(6)	0.4709(10)	1.2362(7)	490(30)	1
C(142)	0.6939(8)	0.4770(12)	1.3312(8)	670(40)	1
C(111)	0.7921(7)	0.2375(7)	1.0662(7)	390(30)	1
C(112)	0.7916(10)	0.1627(9)	0.9913(8)	590(40)	1
O(11)	0.7977(6)	0.2136(5)	0.9071(5)	460(20)	1
C(113)	0.7780(7)	0.3060(7)	0.9289(7)	400(30)	1
C(11A)	0.7221(8)	0.2270(7)	1.1380(9)	480(30)	1
C(12A)	0.6201(8)	0.2264(9)	1.1105(10)	660(40)	1
C(13A)	0.5543(13)	0.2254(11)	1.1766(12)	890(60)	1
C(14A)	0.5922(11)	0.2088(11)	1.2715(10)	710(50)	1
C(15A)	0.6928(15)	0.2035(10)	1.2923(12)	920(70)	1
C(16A)	0.7540(11)	0.2119(10)	1.2283(8)	590(40)	1
C(121)	0.7647(7)	0.3819(6)	0.8572(8)	400(30)	1
C(122)	0.7688(6)	0.3784(7)	0.7646(7)	370(30)	1
C(123)	0.7577(7)	0.4609(9)	0.7154(7)	450(30)	1
C(124)	0.7452(7)	0.5525(7)	0.7562(7)	420(30)	1
C(125)	0.7406(7)	0.5483(7)	0.8472(7)	400(30)	1
O(12)	0.7242(6)	0.7200(5)	0.8856(5)	510(20)	1
C(133)	0.7294(6)	0.6297(7)	0.9154(7)	390(30)	1
C(132)	0.7169(9)	0.7763(7)	0.9750(8)	540(40)	1
C(131)	0.7136(8)	0.7010(7)	1.0520(8)	470(30)	1
C(11B)	0.7905(7)	0.7079(6)	1.1300(8)	410(30)	1
C(12B)	0.7659(10)	0.7127(8)	1.2195(9)	500(40)	1
C(13B)	0.8401(12)	0.7129(9)	1.2967(9)	670(50)	1
C(14B)	0.9334(12)	0.7017(10)	1.2836(9)	770(50)	1
C(15B)	0.9678(9)	0.6910(10)	1.1970(10)	670(50)	1
C(16B)	0.8948(8)	0.6979(7)	1.1230(7)	460(30)	1
Pd(2)	0.7554(1)	0.4872(1)	0.4471(1)	350(10)	1
N(23)	0.9012(5)	0.4865(7)	0.4765(5)	410(20)	1
N(22)	0.7693(6)	0.4899(8)	0.5795(5)	420(20)	1
N(21)	0.6082(5)	0.4940(7)	0.4662(5)	410(20)	1
N(24)	0.7422(6)	0.4816(9)	0.3096(5)	380(30)	1
C(241)	0.7337(7)	0.4890(8)	0.2342(7)	460(30)	1
C(242)	0.7136(8)	0.4970(8)	0.1314(6)	490(30)	1
C(225)	0.8584(6)	0.4890(7)	0.6279(6)	410(30)	1
C(224)	0.8708(8)	0.4931(9)	0.7218(6)	550(30)	1
C(223)	0.7871(7)	0.4961(10)	0.7656(6)	510(30)	1
C(222)	0.6939(7)	0.4990(9)	0.7148(6)	520(30)	1
C(221)	0.6845(7)	0.4883(8)	0.6205(6)	450(30)	1
C(212)	0.4387(7)	0.4827(10)	0.4832(7)	560(40)	1
O(21)	0.5089(4)	0.4961(8)	0.5743(5)	610(30)	1
C(213)	0.6019(6)	0.4910(7)	0.5542(5)	370(20)	1
C(231)	0.9964(7)	0.4712(7)	0.4284(6)	420(30)	1
C(232)	1.0803(8)	0.4690(11)	0.5080(9)	700(50)	1
O(22)	1.0317(5)	0.4790(6)	0.5917(4)	510(20)	1
C(233)	0.9332(6)	0.4837(8)	0.5628(7)	460(30)	1
C(211)	0.5110(6)	0.4998(9)	0.4123(7)	470(30)	1
C(21A)	0.4949(7)	0.4316(8)	0.3310(7)	440(30)	1
C(22A)	0.4903(7)	0.4621(9)	0.2449(7)	500(30)	1
C(23A)	0.4770(8)	0.3959(16)	0.1702(9)	790(60)	1
C(24A)	0.4680(9)	0.3016(16)	0.1852(10)	830(60)	1
C(25A)	0.4731(9)	0.2674(10)	0.2723(11)	660(40)	1
C(26A)	0.4853(7)	0.3313(8)	0.3464(8)	510(30)	1
C(21B)	0.9989(7)	0.5460(9)	0.3542(7)	490(40)	1
C(22B)	1.0165(8)	0.6462(8)	0.3788(9)	560(40)	1
C(23B)	1.0300(9)	0.7097(12)	0.3148(12)	840(60)	1
C(24B)	1.0219(8)	0.6889(15)	0.2200(9)	780(60)	1
C(25B)	1.0002(9)	0.5903(14)	0.1928(10)	790(60)	1

Table 2 (continued)

Atom	x	y	z	$U_{iso/equiv}$	Occupancy factor
C(26B)	0.9898(7)	0.5201(10)	0.2619(8)	550(40)	
B(11)	0.7689(6)	−0.2590(6)	0.5606(5)	430(30)	1
F(11)	0.6844(5)	−0.3042(5)	0.5231(5)	840(30)	1
F(12)	0.8436(5)	−0.2843(6)	0.5115(5)	880(30)	1
F(13)	0.7925(7)	−0.2884(6)	0.6498(4)	950(40)	1
F(14)	0.7552(5)	−0.1611(4)	0.5572(4)	600(20)	1
B(21)	0.5325(6)	0.5345(6)	0.9164(5)	440(20)	1
F(21)	0.6332(4)	0.5349(6)	0.9217(5)	840(30)	1
F(22)	0.5033(7)	0.4518(5)	0.9562(5)	930(40)	1
F(23)	0.4933(5)	0.5362(7)	0.8256(4)	860(30)	1
F(24)	0.5002(7)	0.6109(6)	0.9602(6)	1020(40)	1
B(4)	0.9781(7)	0.4448(8)	0.9745(7)	940(60)	1
F(41)	1.0293(7)	0.5196(11)	0.9450(12)	2550(130)	1
F(42)	1.0270(5)	0.4081(6)	1.0534(5)	890(30)	1
F(43)	0.9687(10)	0.3737(11)	0.9106(8)	2210(90)	1
F(44)	0.8862(4)	0.4770(5)	0.9881(5)	680(20)	1
B(3)	0.2788(8)	−0.2711(7)	0.4692(7)	670(40)	1
F(31)	0.3312(15)	−0.2428(13)	0.4021(11)	1230(190)	0.39(7)
F(32)	0.2509(5)	−0.3645(5)	0.4591(5)	700(20)	1
F(33)	0.1955(9)	−0.2146(8)	0.4687(10)	1090(70)	0.70(4)
F(34)	0.3317(8)	−0.2586(8)	0.5534(7)	1340(70)	0.98(4)
F(35)	0.2758(22)	−0.2298(17)	0.3836(11)	970(110)	0.45(5)
F(36)	0.3754(17)	−0.2863(44)	0.4566(46)	3000(420)	0.61(9)

lar to the coordination plane. The angles between these two rings and the plane defined by the Pd^{II} and the four donor N-atoms are 79° and 76° for the 'a' and 'b' rings, respectively. Consequently, the acetonitrile methyl group is relatively close to the π-clouds (shielding regions) of these benzene rings and this affects their methyl proton chemical shifts.

The FAB mass spectra of the complexes **5–8** show relatively intense peaks for the $[Pd(pybox)]^{2+}$ dication and for the **fluoride**-extracted monocation $[PdF(pybox)]^{+}$ (see Fig. 2). Obviously, the BF_4^- serves as a source of the fluoride ion which, after loss of CH_3CN, coordinates to the Pd^{II}. We did not detect a higher molecular weight ion with a coordinated acetonitrile in **5–8**.

The IR spectra show the coordinated acetonitrile at 2332 cm^{-1}, 2342 cm^{-1}, 2332 cm^{-1} and 2346 cm^{-1} for **5–8**, respectively, with $[Pd(CH_3CN)_4]^{2+}$ at 2333 cm^{-1} and CH_3CN at 2255 cm^{-1}. In the model complexes **9–13**, some of which contain chiral auxiliaries, e.g.

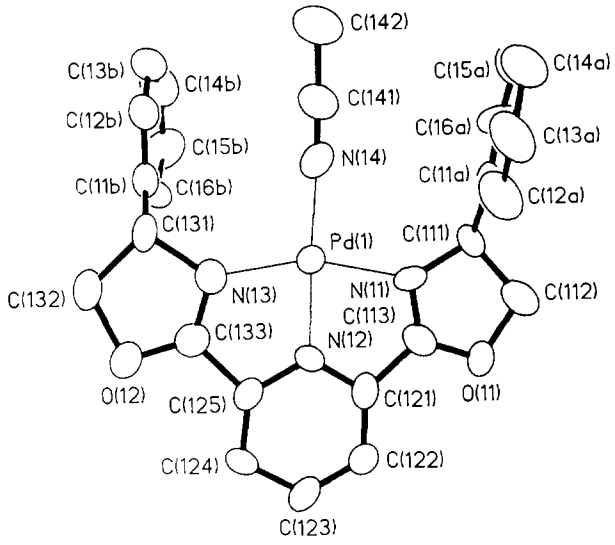

Fig. 1. ORTEP plot of the cation of **6**.

Table 3
Selected bond lengths (Å) and bond angles (°) for **6** and **21g**

	6	**21g**
Pd(1)–N(11)	2.029(9)	2.065(9)
Pd(1)–N(12)	1.925(7)	2.023(10)
Pd(1)–N(13)	1.987(8)	2.066(9)
N(13)–C(133)	1.274(14)	1.261(15)
N(11)–C(113)	1.243(13)	1.317(15)
N(14)–C(141)	1.163(14)	
Pd(1)–N(14)	1.968(9)	
Pd–P		2.296(3)
N(11)–Pd(1)–N(12)	79.4(4)	78.8(4)
N(11)–Pd(1)–N(13)	159.7(3)	156.3(4)
N(12)–Pd(1)–N(13)	80.7(5)	77.5(4)
N(11)–Pd(1)–N(14)	99.0(5)	
N(11)–Pd–P		103.2(3)
N(13)–Pd–P		100.4(3)
N(12)–Pd–P		175.0(3)
N(12)–Pd(1)–N(14)	176.3(5)	
Pd(1)–N(14)–C(141)	170.7(8)	
N(13)–Pd(1)–N(14)	101.3(5)	
N(14)–C(141)–C(142)	178.6(14)	
P–C(111P)		1.804(12)
P–C(121P)		1.785(11)
P–C(131P)		1.813(12)

Table 4
^1H and ^{13}C NMR data[a] for the CH_3 group of the complexed CH_3CN

Compound	$\delta(CH_3)$ (ppm)	$\delta(CH_3)$ (ppm)
CH_3CN	2.01	1.4
$[Pd(CH_3CN)_4]^{2+}$	2.62 (2.65 [b])	
5	2.68	3.7
6	1.88	2.7
7	2.53	4.1
8	2.01	2.9
9	1.93	2.2
10	1.90	2.1
11	1.84	1.9
12	2.75	4.0
13	2.59	3.7
$[Pd(terpy)(CH_3CN)]^{2+}$ [c]	2.83	4.0

[a] CD_3NO_2 solutions, rel. to TMS. [b] From Ref. [10]. [c] See Ref. [3].

BINAP, there are strong C–N stretching bands in the same region (see Scheme 2). Since acetonitrile complexes are useful starting materials, we have prepared and isolated **9–13** and give data for these under Experimental details.

The CH_3CN complexes **5–13** afford ^1H and ^{13}C NMR spectra which are consistent with their formulations. The coordinated CH_3CN ligands show ^1H-methyl resonances at both lower and higher frequencies relative to the free ligand (see Table 4). The high frequency values, $\delta = 2.53$–2.83 ppm, $\Delta\delta = 0.52$–0.82 ppm, are found for most of the complexes with a nitrogen donor trans to CH_3CN. This change is, presumably, due to coordination and the consequent flow of electron from the acetonitrile to the Pd^{II}. The low-frequency shifts, $\delta = 1.84$–2.01 ppm, $\Delta\delta = 0$ to -0.17 ppm, are found for complexes with a phosphorus donor trans to CH_3CN. These shifts are partially anisotropic in origin and arise due to the presence of a *cis*-aromatic ring, e.g., for **6**, $\delta(CH_3CN) = 1.88$ ppm.

2.3. Isonitrile complexes

Since the condensation reaction of Eq. (1) requires isonitrile coordination to Pd^{II}, we prepared the isonitrile complexes **14–16** with $CNCH_2COOMe$ (see Scheme 3). In contrast to the pybox complexes **5–8**, which are yellow–orange in colour, these pybox-isonitrile derivatives are blue in colour. The yields of **14–16** are excellent (83%–97%) and the complexes could be characterised as with **5–8**. We note that the ^{13}C signal for the isonitrile CH_2 in coordinated $CNCH_2CO_2Me$ shows a ca. 17 Hz ^{14}N coupling.

As the catalytic reaction in Eq. (1) requires an excess of isonitrile, we followed the change in the ^1H spectrum of the CH_3CN complex **7** upon stepwise addition of CN^tBu in CD_3CN solution. The ^tBu derivative was chosen as its ^1H-^tBu resonance is remote from those of the oxazoline resonances. Interestingly, after initial formation of a compound which we assumed to be the CN^tBu analogue of **16** (1 equiv. of isonitrile added), addition of eight further equivalents results in the formation of proton signals attributable to **uncoordinated** pybox **7** and a new ^tBu singlet at 1.56 ppm. Addition of ether to the NMR tube induced precipitation of a white powder. Work-up of this powder and a subsequent ^1H NMR spectrum reveals only the singlet at 1.56 ppm. As there is no longer a complexed pybox ligand, we assumed that $[Pd(CN^tBu)_4](BF_4)_2$ (**17**) had been generated and could confirm this via an independent synthesis. The FAB mass spectrum of **17** has a strong peak (35% of base) at $m/e = 524$, which we assign to the mono-BF_4^- cation $\{[Pd(CN^tBu)_4](BF_4)\}^+$. The analogous tetrakis-isonitrile complex $[Pd(CNCH_2COOMe)_4)](BF_4)_2$ (**18**) was also prepared.

The ineffectiveness of the chiral pybox ligands in terms of enantioselectivity is now clear. However, in the

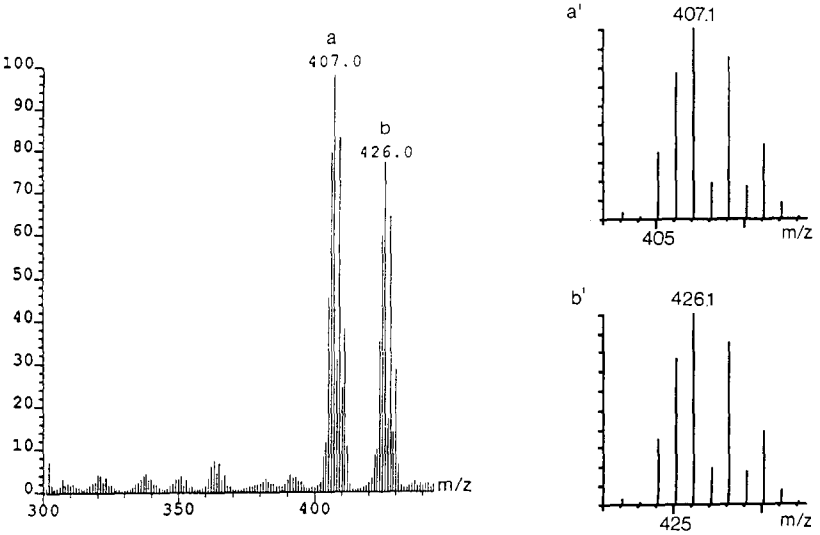

Fig. 2. FAB mass spectrum in the high molecular weight region of **5** with expansions of the two most intense groupings at $m/e = 407$, $[Pd(\mathbf{1})]^{2+}$ and $m/e = 426$, $[PdF(\mathbf{1})]^+$ The latter arises from the extraction of F^- from BF_4^-.

presence of chiral ferrocene diphosphine ligands containing a chiral amine side-chain, substantial enantiomeric excesses have been found [4,5]. Consequently, we prepared the model ferrocene bis-phosphine bis-isonitrile dication, **19**. After measuring its ^{31}P spectrum, **19** was dissolved in CD_3CN and treated with 100 equiv. of CN^tBu. The ^{31}P spectrum of the resulting solution (and of a solution with 100 equiv. of CN^tBu in $CDCl_3$) revealed **19** to be the only observable complex. Clearly, whereas a ferrocene diphosphine can compete favourably against excess CN^tBu for Pd^{II}, a pybox nitrogen tridentate donor cannot.

2.4. *[Pd(L)(3)]$^{n+}$ complexes*

Given the somewhat unexpected loss of pybox in the isonitrile chemistry, we thought it useful to prepare and characterise additional [Pd(ligand)(pybox)]$^{n+}$ cationic complexes. The ligands were chosen so as to reflect a variety of different electronic and steric possibilities, and these products, **21a–j**, derived from **7**, are shown in Scheme 4. Of the L-ligands, perhaps the formate, **21i**, is the most interesting in that the Pd–OCHO [11] and

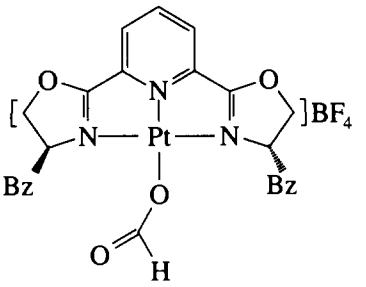

(21i)

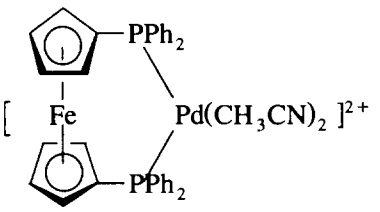

(9)

1,1′-Bis(diphenylphosphino)ferrocene complex 2325 cm^{-1}

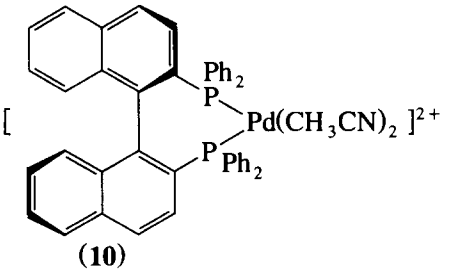

(10)

(*R*)-Binap complex 2325 cm^{-1}

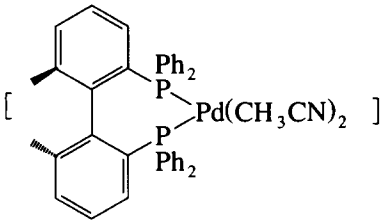

(11)

(*S*)-Biphemp complex 2320 cm^{-1}

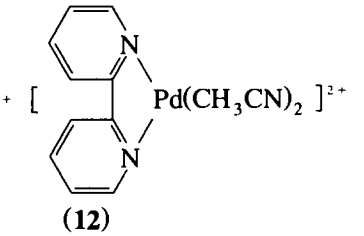

(12)

2,2′-Bipyridyl complex 2332 cm^{-1}

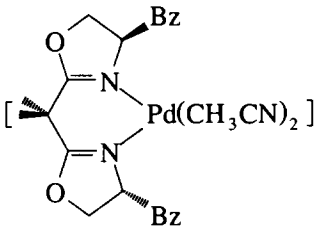

(13)

2,2-Bis-[(*R*)-4′-(benzyl)oxazoline-2′-yl]propane 2339 cm^{-1}

5 = 2322 cm^{-1}
6 = 2342 cm^{-1}
7 = 2332 cm^{-1}
8 = 2346 cm^{-1}

Scheme 2. Some IR data for model complexes.

Pt–OCHO [12] fragments are sources of the hydride ligand. We find the ^{1}H and ^{13}C chemical shifts for **21i** to be 7.74 and 169.9 ppm, respectively (and for the Ph–pybox formate analogue, 6.61 and 168.6 ppm, respectively). Our measured carbon values are within 3 ppm of those found by Oshima et al. [11] in their π–allyl complexes; however, our ^{1}H shifts are at much lower frequency than theirs; 8.82–8.98 ppm.

The chemical shifts of the *para*-pyridine protons in **21** are of potential interest in that they might reflect how the pybox responds electronically to the different ligands L. Generally, there is a high-frequency shift upon coordination, $\Delta\delta = 0.53–0.79$ ppm, presumably as a consequence of some contribution of the resonance structure shown in scheme 4; however, the $\Delta\delta$ does not seem to be related to the donor strength of L, i.e., the chemical shift is independent of the trans influence of the ligand L. As an example, we note that the δ value for **7** (CH_3CN), 8.63 ppm, is close to that for **21g** (PPh_3), 8.64 ppm.

We were especially curious to see if and how large ligands would fit into the chiral pocket. For the 2,6-dimethypyridine complex **21b**, we find that the pybox benzyl protons $H_7^{pro\text{-}R}$ and $H_7^{pro\text{-}S}$, are shifted to lower frequency, $\delta = 2.28$ and 2.79 ppm, due to the anisotropy of the lutidine ring (free ligand signals are located at $\delta = 2.74$ and 3.27 ppm), so that this ring must lie approximately perpendicular to the coordination plane. In the ^{1}H NOESY for **21b**, the equivalent 2,6-methyl groups show moderate and almost equivalent NOEs to **both** of the diastereotopic benzyl CH_2-protons as well as to the *ortho*-protons of the Bz group. Obviously, the benzyl groups have quite a bit of freedom so that there

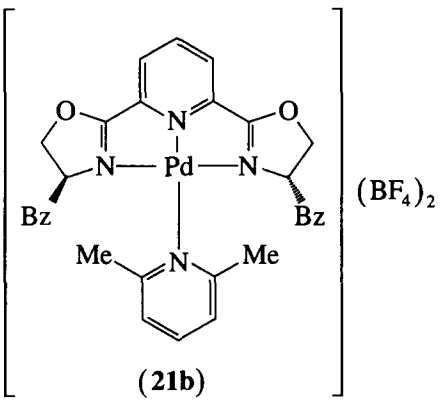

(21b)

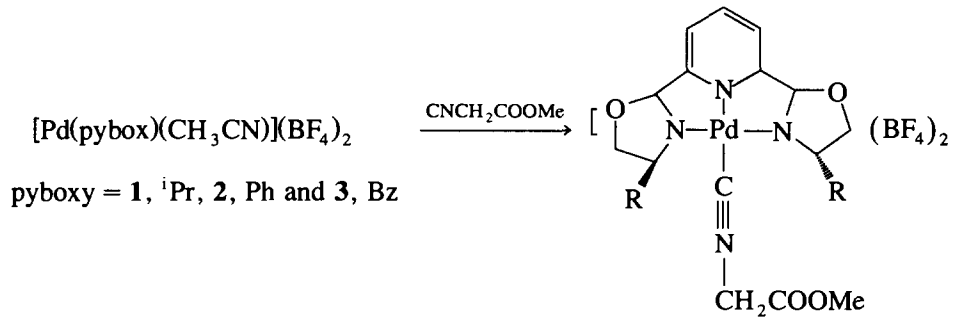

(14) R = ^{i}Pr

(15) R = Ph

(16) R = Bz

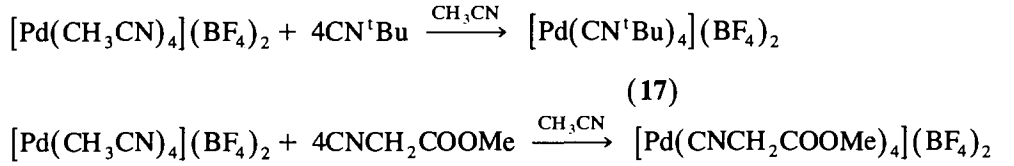

(17)

(18)

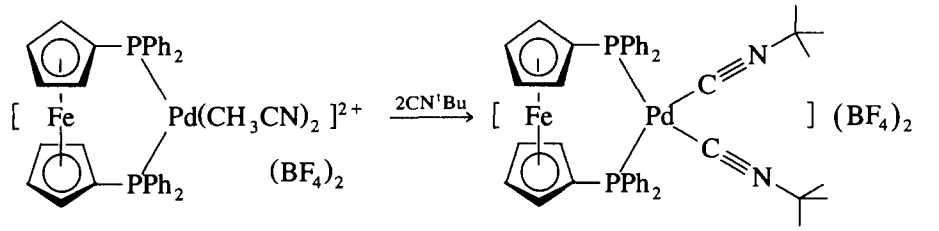

(19)

Scheme 3. Isonitrile reactions.

$7 + L \longrightarrow [Pd(L)(\mathbf{3})]^{n+}(BF_4)_n$ (**21**) $+ CH_3CN$	δ^1H (ppm)
L = **a**, 4-methylpyridine	8.67
b, 2,6-dimethylpyridine	8.69
c, 4-methyl aniline	8.59
d, $H_2NCH_2CH(OMe)_2$	8.58
e, $H_2NCH_2CH_2OH$	8.59
f, $H_2N(CH_2)_5CH_3$	8.64
g, PPh_3	8.64
h, N_3^-	8.50
i, HCO_2^-	8.43
j, Cl^-	8.46
k, $CH_2 = CHCN$	8.61
complex **7** (CH_3CN)	8.63
ligand **3**	7.90

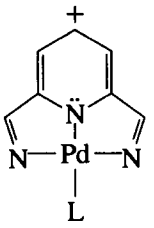

resonance structure for a fragment of **21** with a positive charge on the *para* carbon.

Scheme 4. Complexes **21** of the Bz pybox **3** and their ^{1}H *para*-pyridine proton chemical shifts.

seem to be no major problems in coordinating this bulky pyridine.

Since the 2,6-dimethylpyridine can slip in sideways, we made **21g**, with the larger PPh_3 ligand, and have determined its structure by X-ray diffraction. An ORTEP plot of this molecule is given in Fig. 3 and experimental details of the structure and positional parameters are given in Tables 1 and 5, respectively. Selected bond lengths and bond angles are also to be found in Table 3, to facilitate a comparison with **6**.

It is clear from the ORTEP that sufficient space can be made to accommodate the relatively large PPh_3 ligand. Still, this space is obtained at the price of some distortions within the Pd coordination sphere. The local geometry about the Pd atom is distorted square-planar, with the Pd atom about 0.049 Å **below** the coordination

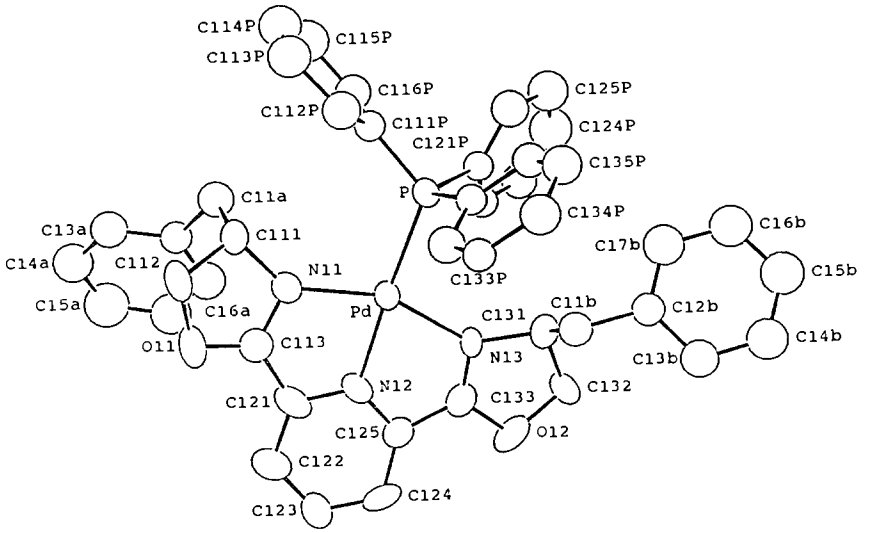

Fig. 3. ORTEP plot of the cation of **21g**.

Table 5
Final positional and isotropic equivalent displacement parameters for **21g** (esds given in parentheses)

Atom	x	y	z	B (Å²) [a]
Pd	0.04252(6)	−0.00543(4)	0.10476(3)	2.44(1)
P	0.0419(3)	0.0686(1)	0.1885(1)	2.72(5)
O11	0.2506(7)	0.0614(4)	−0.0351(3)	4.1(2)
O12	−0.2037(6)	−0.1902(4)	0.0895(3)	4.3(2)
N11	0.1782(7)	0.0498(5)	0.0549(4)	2.8(2)
N12	0.0286(7)	−0.0665(5)	0.0297(3)	2.8(2)
N13	−0.1020(7)	−0.0850(5)	0.1229(3)	2.7(2)
C111	0.273(1)	0.1144(6)	0.0588(5)	3.6(2)
C112	0.288(1)	0.1335(7)	−0.0055(5)	4.1(3)
C113	0.1781(9)	0.0243(6)	0.0019(4)	3.1(2)
C11a	0.394(1)	0.0845(7)	0.0893(5)	4.3(2) *
C12a	0.472(1)	0.0277(6)	0.0556(5)	3.7(2) *
C13a	0.579(1)	0.0549(7)	0.0251(5)	4.6(3) *
C14a	0.650(1)	0.0057(9)	−0.0076(5)	5.2(2) *
C15a	0.613(1)	−0.0744(9)	−0.0117(6)	6.5(3) *
C16a	0.513(1)	−0.1012(8)	0.0162(6)	6.1(3) *
C17a	0.440(1)	−0.0521(7)	0.0503(5)	4.7(3) *
C121	0.1029(9)	−0.0459(6)	−0.0143(4)	3.2(2)
C122	0.091(1)	−0.0841(8)	−0.0650(5)	4.3(3)
C123	0.011(1)	−0.1463(7)	−0.0706(5)	4.1(3)
C124	−0.069(1)	−0.1690(6)	−0.0257(5)	4.6(3)
C125	−0.050(1)	−0.1269(6)	0.0252(4)	3.3(2)
C131	−0.2011(9)	−0.1016(6)	0.1673(5)	3.3(2)
C132	−0.241(1)	−0.1852(7)	0.1485(5)	4.5(3)
C133	−0.1206(9)	−0.1339(6)	0.0809(5)	3.1(2)
C11b	−0.304(1)	−0.0389(7)	0.1670(5)	4.0(2) *
C12b	−0.395(1)	−0.0471(6)	0.2147(5)	3.1(2) *
C13b	−0.512(1)	−0.0825(7)	0.2075(5)	4.5(3) *
C14b	−0.598(1)	−0.0918(8)	0.2533(6)	5.1(3) *
C15b	−0.560(1)	−0.0696(8)	0.3059(6)	5.7(3) *
C16b	−0.441(1)	−0.0377(7)	0.3168(6)	5.4(3) *
C17b	−0.362(1)	−0.0263(8)	0.2700(6)	5.7(3) *
C111P	0.1668(9)	0.1397(6)	0.2011(4)	2.9(2) *
C112P	0.162(1)	0.2136(7)	0.1800(5)	4.4(2) *
C113P	0.265(1)	0.2685(8)	0.1897(6)	5.7(3) *
C114P	0.359(1)	0.2434(9)	0.2194(6)	5.6(3) *
C115P	0.373(1)	0.1682(8)	0.2404(6)	6.0(3) *
C116P	0.273(1)	0.1114(7)	0.2332(6)	4.6(3) *
C121P	0.0400(9)	0.0071(6)	0.2522(4)	2.9(1) *
C122P	0.0594(9)	−0.0727(6)	0.2472(4)	3.3(2) *
C123P	0.063(1)	−0.1225(7)	0.2961(5)	4.3(2) *
C124P	0.050(1)	−0.0895(8)	0.3489(6)	6.1(3) *
C125P	0.034(1)	−0.0125(7)	0.3553(5)	5.3(2) *
C126P	0.031(1)	0.0400(7)	0.3063(5)	4.6(2) *
C131P	−0.0996(9)	0.1274(6)	0.1839(4)	2.8(2) *
C132P	−0.139(1)	0.1518(7)	0.1304(5)	4.0(2) *
C133P	−0.2496(9)	0.1976(6)	0.1223(4)	3.3(2) *
C134P	−0.317(1)	0.2218(7)	0.1704(5)	4.5(3) *
C135P	−0.274(1)	0.1984(7)	0.2246(5)	4.3(2) *
C136P	−0.173(1)	0.1530(7)	0.2315(5)	3.6(2) *
F1	−0.051(1)	0.0950(6)	−0.0303(5)	9.5(3) *
F2	−0.001(1)	0.2135(7)	0.0128(5)	9.9(3) *
F3	0.495(1)	0.302(1)	0.0821(7)	14.3(5) *
F4	−0.183(1)	0.1952(8)	−0.0332(5)	10.0(3) *
B1	−0.053(2)	0.172(1)	−0.0326(9)	6.8(4) *
F5	−0.2507(9)	−0.2038(7)	−0.1321(4)	9.4(3) *
F6	−0.3149(9)	−0.2794(6)	−0.0592(4)	8.0(2) *
F7	0.213(1)	−0.1573(8)	0.1388(5)	11.7(3) *
F8	0.074(1)	−0.2419(7)	0.1417(5)	10.4(3) *
B2	−0.316(2)	−0.265(1)	−0.1124(9)	6.5(4) *

[a] Starred atoms were refined isotropically. Anisotropically refined atoms are given in the form of the isotropic equivalent displacement parameter defined as: $(4/3)[a^2B_{1,1} + b^2B_{2,2} + c^2B_{3,3} + ab(\cos\gamma)B_{1,2} + ac(\cos\beta)B_{1,3} + bc(\cos\alpha)B_{2,3}]$.

plane defined by the four donors and the metal, whereas the N(12) and P atoms are ca. 0.040 Å and 0.031 Å, respectively, **above** this plane. The corresponding values in **6** were 0.026 Å, 0.029 Å and 0.024 Å for the Pd, N(12) and N(14), respectively, i.e., planarity within the coordination sphere is more difficult for **21g** than for **6**.

In **21g** the N(11)–Pd–N(13) angle, at 156.3(4)°, is even smaller than that for **6**, 159.7(3)°, thereby 'opening' the front of the molecule even further. The Pd–P bond length, 2.296(3) Å, is longer than expected for the trans arrangement N(12)–Pd–P, e.g., in *trans*-$PdCl_2$(2-methylpyridine)(PEt_3) [13], the Pd–P separation is 2.228(2) Å. In *trans*-$PdCl_2(PPh_3)_2$ [14] (P trans to P), the Pd–P separation is 2.337(1) Å, so that the 2.298(3) Å value for **21g** is, indeed, somewhat long. The Pd–N(12) bond length in **21g**, 2.019(7) Å, is almost 0.1 Å longer than in **6** but comparable with the Pd–N distance in the bis-oxazole compound *trans*-$PdCl_2(oxazole)_2$ [15], 2.016(2) Å. Interestingly, in a terpyridine, phenylcyanamide palladium complex [16] (with two fused five-membered rings), one finds the central terpyridine N–Pd separation at 1.932(4) Å, in agreement with what we observe in **6**. It would seem that the PPh_3 ligand is not lengthening the Pd–N(12) bond nearly as much as in *trans*-$PdCl_2$(2-methylpyridine)(PEt_3) [13], whose Pd–N bond length is 2.155(5) Å.

It is curious that while the benzyl group at C(131) in **21g** is placed away from the oxazoline, the benzyl at C(111) tucks down and toward its oxazoline. The angle between the planes defined by the phenyl of the benzyl at C(111) and the oxazoline ring with N(11) is about 45°. We presume that steric effects are responsible for this difference. Concluding, it would seem that the Pd–pybox fragment can accommodate various ligands in the fourth position; however, for a large ligand, some angles and distances are distorted.

We have also attempted to prepare NEt_3 and H_2N^tBu analogues; however, these gave mixtures of products. We suspect that the increased basicity of these two, $pK_a = 11.01$ and 10.96, respectively, may have induced competition reactions arising from serendipitous water. Palladium(II) complexes with bridging OH ligands are known [8,17]; indeed the structure of [Pd(terpy)(OH)]-$ClO_4 \cdot H_2O$ has been determined [8].

2.5. Summary

We have prepared a series of new chiral cationic complexes of Pd^{II} with several tridentate nitrogen-pybox ligands. A variety of ligand types can occupy the fourth coordination position. The coordinated pybox ligand can distort so as to open the fourth coordination position sufficiently to allow complexation of bulky ligands. However, in the presence of an excess of isonitrile, the chiral tridentate is completely displaced from the palladium, thereby rendering these pybox ligands useless as chiral auxiliaries in the aldol reaction of $CN_2CH_2CO_2$-Me with PhCHO.

3. Experimental details

IR spectra were measured on a Perkin-Elmer 883 instrument. FAB mass spectra and microanalyses were performed in the analytical laboratories of the ETH Zürich. NMR spectra were measured as CD_3NO_2 (and sometimes $CDCl_3$) solutions using Bruker AC-250 and AMX-500 spectrometers. Conductivity measurements were made in nitromethane.

3.1. Crystal structure determination of [6](BF$_4$)$_2$

Crystals suitable for diffraction were obtained from acetonitrile/ether solution and measured on an X-ray scanner (STOE/IPDS) using 7104 observed reflections of the 15 051 measured reflections for the determination and the refinement of the structure. The systematic extinctions are consistent with the space groups $P2_1/m$ and $P2_1$, both of which have been tested for a structural solution. The refined final acentric model shows that a centrosymmetric description of the structure is not probable. This is mainly due to the distribution of the BF_4^- anions and the organic side-chain of the cation. Only the central positions of the Pd complex come close to the mirror symmetry. Further, it is not possible to map the two molecules on top of each other by an inversion centre without severe deviations. Consequently, the free refinement by the full-matrix least squares in the acentric space groups yields correlation matrix elements < 0.55.

Isotropic and anisotropic displacement parameters are in the normal range for all atoms except for some of the fluorines which form split positions at the sites of the disordered BF_4^- anions. The hydrogen positions have been calculated by geometrical considerations. Inspection of the interatomic distances shows that the H-positions fit well into the pattern of the heavier atoms. The largest residual peak in the final difference Fourier synthesis is about 1.3 e A^3 high and belongs to the region of a BF_4^- group (B4). The final list of differences, $F_{obs} - F_{calc}$ does not show any systematic trends or extreme values.

3.2. Crystal structure determination of [21g](BF$_4$)$_2$

Crystals suitable for diffraction were obtained from acetonitrile/ether solution and then mounted on a glass fibre on an Enraf-Nonius CAD4 diffractometer for the unit cell and space group determinations and for the data collection. Unit cell dimensions were obtained by least-squares fit of the 2θ values of 25 high-order reflections. Data were collected with variable scan speed

to ensure constant statistical precision on the collected intensities. Three standard reflections were used to check both the stability of the crystal and of the experimental conditions, and measured every hour. The orientation of the crystal was checked by measuring three reflections every 300 measurements. Data have been corrected for Lorentz and polarization effects using the data reduction programs of the MOLEN package [18]. Empirical adsorption corrections were applied by using azimuthal (ψ) scans of three 'high-χ' angles. The standard deviations on intensities were calculated in terms of statistics alone, while those on F_0 were calculated as shown in Table 1. The structures were solved by a combination of Patterson and Fourier methods and refined by full-matrix least-squares [18] (the function minimized being $\Sigma[w(F_o - 1/kF_c)^2]$).

Anisotropic displacement parameters were used for the Pd,P atoms and those of the pybox ligand while the others have been treated isotropically. No extinction correction was found to be necessary. The scattering factors used, corrected for the real and imaginary parts of the anomalous dispersion [19], were taken from Ref. [19].

The handedness of the structure was tested by refining both sets of coordinates. Those giving the significantly lower R_w factor (0.062 versus 0.068) were used [20]. All calculations were carried out using the Enraf-Nonius MOLEN package [18]. The contribution of the hydrogen atoms in calculated positions [C=H = 0.95 (Å), B(H) = 1.3 × B(C-bonded) (Å^2)] was taken into account but not refined.

Final atomic coordinates and equivalent isotropic displacement parameters are given in Table 5.

Ligands **1–3** hae been prepared previously [3,6].

3.3. Synthesis of 2,6-bis[4'-(R)-(p-EtOPh)-oxazoline-2'-yl]pyridine, (R,R)-p-EtOPh-pybox (6)

3.3.1. (R)-(p-EtOPh)glycine

(*R*)-(*p*-Hydroxyphenyl)glycine (24.93 g, 149.0 mmol), 500 ml of dimethyl sulphoxide and a solution of NaOH (11.92 g, 298.0 mmol) in 100 ml of water was warmed at 80°C until a solution was obtained. The temperature was then reduced to 60°C and the solution treated with ethyl iodide (12.17 ml, 149.0 mmol). Stirring for 15 h at this temperature was followed by addition of 300 g of ice. Reduction of the pH to 7.5 with dil. HCl afforded a white precipitate which was filtered and washed with water. Recrystallisations from 60% acetic acid gave 3.78 g (13%) of (*R*)-(*p*-ethoxyphenyl)glycine as white crystals. ^{1}H NMR (CD_3CO-OD)δ: 1.41 (t, J = 7.0 Hz, 3H); 4.08 (q, J = 7.0 Hz, 2H); 5.19 (s, 1H); 6.96 (d, J = 8.6 Hz, 2H); 7.43 (d, J = 8.6 Hz, 2H) ppm. ^{13}C NMR (CD_3COOD)δ: 16.0; 59.7; 65.7; 117.1; 126.9; 131.9; 162.0; 172.9 ppm. Analysis: Calc. for $C_{10}H_{13}NO_3$ (195.22): C, 61.53; H, 6.71; N, 7.17%. Found: C, 61.31; H, 6.63; N, 7.13%.

3.3.2. (R)-2-(p-EtOph)glycinol

(*R*)-(*p*-Hydroxyphenyl)glycine (2.81 g, 14.4 mmol) was reacted with $LiAlH_4$ (1.37 g, 36.0 mmol) in 150 ml abs. THF at reflux for 6 h. Careful destruction of the excess hydride was followed by filtration and washing with ether. Solution in methanol and filtration to remove futher salts was followed by removal of the methanol. The product, 2.14 g (82%) of (*R*)-2-(*p*-Ethoxyhenyl)glycinol, is a white powder whose ^{1}H spectrum showed no impurities. ^{1}H NMR (CD_3OD)δ: 1.44 (t, J = 7.0 Hz, 3H); 3.57 (dd, J = 10.7, 8.3 Hz, 1H); 3.72 (dd, J = 10.7, 4.6 Hz, 1H); 3.96 (dd, J = 8.3, 4.6 Hz, 1H); 4.09 (q, J = 7.0 Hz, 2H); 6.94 (d, J = 8.7 Hz, 2H); 7.33 (d, J = 8.7 Hz, 2H) ppm. ^{13}C NMR ($CDCl_3$)δ: 15.9; 59.0; 65.3; 69.9; 116.3; 129.7; 136.2; 160.5 ppm.

3.3.3. (R,R)-p-EtOPh-pybox · 2HCl

(*R*)-2-(*p*-Ethoxyphenyl)glycinol (1.31 g, 7.2 mmol) was dissolved in 30 ml of $CHCl_3$ under an N_2 atmosphere. The solution was cooled with an ice bath and treated slowly with pyridine-2,6-dicarbonylchloride (0.71 g, 3.5 mmol) in 5 ml of $CHCl_3$. After 5 min, the reaction mixture was treated dropwise with 2.9 ml of triethylamine (2.9 ml, 21.0 mmol) and allowed to stir for 24 h. Careful addition of 3.3 ml of thionyl chloride was followed by refluxing for 2 h. After cooling to room temperature, the reaction mixture was treated **carefully** with water to destroy the excess thionyl chloride. Treatment with 10 ml of 0.1 M K_2CO_3 and then 20 ml of water was followed by separation of the organic layer and drying over $MgSO_4$. Removal of the solvent and column chromatography (R_f = 0.7, CH_2Cl_2/Ether = 3 : 2) afforded 1.45 g (78%) of product as the dihydrochloride; $[\alpha]_D^{22}$ = 104.7° (c = 0.40, $CHCl_3$). ^{1}H NMR ($CDCl_3$)δ: 1.41 (t, J = 7.0 Hz, 6H); 3.9–4.0 (m, 4H); 4.02 (q, J = 7.0 Hz, 4H); 5.4–5.6 (m, 2H); 6.90 (d, J = 8.7 Hz, 4H); 7.32 (d, J = 8.7 Hz, 4H); 8.06 (t, J = 7.8 Hz, 1H); 8.36 (d, J = 7.8 Hz, 2H); 8.43 (d, J = 8.1 Hz, 2H) ppm. ^{13}C NMR ($CDCl_3$)δ: 14.5; 48.1; 52.8; 63.2; 114.5; 125.0; 127.5; 129.8; 139.0; 148.1; 158.6; 162.4 ppm. Analysis: Calc. for $C_{27}H_{29}N_3O_4Cl_2$ (530.45). C, 61.14; H, 5.51; N, 7.92%. Found: C, 60.66; H, 5.48; N, 7.83%.

3.3.4. (R,R)-p-EtOPh-pybox (4)

The dihydrochloride (1.45 g, 2.7 mmol) was dissolved in 30 ml CH_2Cl_2, then treated with a solution of NaC^{t}Bu (0.79 g, 8.2 mmol) in 30 ml of MeOH and stirred for 5 d at room temperature. Addition of 100 ml of H_2O and the same amount of CH_2Cl_2 was followed by separation of the phases, drying of the organic layer over $MgSO_4$ and solvent distillation. Recrystallisation

from CH_2Cl_2 (minimum amount)/hexane and washing with ether afforded 1.07 g (86%) of **4** as a white solid; m.p. 177°C; $[\alpha]_D^{22} = 202.6°$ ($c = 0.99$, CH_2Cl_2). IR (KBr) cm^{-1}: 1637 s; 1377 (s); 1254 (s); 1104 (s); 834 (s). ^1H NMR ($CDCl_3$)δ: 1.41 (t, $J = 7.0$ Hz, 6H); 4.03 (q, $J = 7.0$ Hz, 4H); 4.40 (t, $J = 8.6$ Hz, 2H); 4.89 (dd, $J = 10.2$, 8.6 Hz, 2H); 5.40 (dd, $J = 10.2$, 8.6 Hz, 2H); 7.90 (t, $J = 7.8$ Hz, 1H); 8.33 (d, $J = 7.8$ Hz, 2H) ppm. ^{13}C NMR ($CDCl_3$)δ: 14.5; 63.2; 69.6; 75.2; 114.5; 125.9; 127.6; 133.5; 137.0; 146.6; 158.3; 162.9. MS (El) *m/e*: 457 (36); 162 (24); 148 (100); 135 (19); 120 (25); 107 (15); 78 (9). Analysis: Calc. for $C_{27}H_{23}N_3O_4$ (457.53): C, 70.88; H, 5.95; N, 9.18%. Found: C, 70.15; H, 6.06; N, 9.08%.

Details of the preparation of the mono-acetonitrile complexes (and specifically those for **5** and **7**) have been reported previously [3]. We give results below for the new analogues.

3.4. Synthesis of [Pd((S,S)-Ph-pybox)(CH_3CN)](BF_4)$_2$ (6)

[Pd(CH_3CN)$_4$](BF_4)$_2$ [7] (84.7 mg, 1.91×10^{-4} mol) and **2** (70.5 mg, 1.91×10^{-4} mol) in 5 ml of acetonitrile afforded 138.3 mg (93%) of **6** as a yellow solid. Recrystallisation from CH_3CN/ether gave crystals suitable for X-ray analysis; m.p. 25°C (decomp.); $[\alpha]_D^{20} = 284.6°$ ($c = 1.03$, CH_3NO_2). IR (CsI) (cm^{-1}): 2342 (m); 2317 (m). ^1H NMR (CD_3NO_2): 1.88 (s, 3H); 5.00 (t, $J = 8.7$ Hz, 2H); 5.49 (dd, $J = 10.6$, 8.7 Hz, 2H); 5.60 (dd, $J = 10.6$, 8.7 Hz, 2H); 7.48 (s, 10H); 8.29 (d, $J = 8.1$ Hz, 2H); 8.74 (t, $J = 8.1$ Hz, 1H) ppm. ^{13}C NMR (CD_3NO_2)δ: 2.7; 68.1; 82.3; 126.7; 129.5; 130.3; 130.7; 131.2; 137.8; 146.7; 147.6; 172.3. MS (FAB)*m/e*: 494 (35); 475 (100). Analysis: Calc. for $C_{29}H_{22}N_4O_2B_2F_8Pd$ (690.49): C, 43.49; H, 3.21; N, 8.11%. Found: C, 43.41; H, 3.40; N, 7.99%.

3.5. Synthesis of [Pd((R,R)-p-EtOPh-pybox)(CH_3CN)](BF_4)$_2$ (8)

[Pd(CH_3CN)$_4$(BF_4)$_2$ (25.6 mg, 5.77×10^{-5} mol) and **4** (26.4 mg, 5.77×10^{-5} mol) in 5 ml of acetonitrile afforded 42.5 mg (94%) of **8** as a yellow solid; m.p. 156°C (decomp.); $[\alpha]_D^{22} = -347.7°$ ($c = 0.96$, CH_3NO_2). IR (CsI) (cm^{-1}): 2346 (m); 2320 (m) ^1H NMR (CD_3NO_2) δ: 1.35 (t, $J = 7.0$ Hz, 6H); 2.01 (s, 3H); 4.06 (q, $J = 7.0$ Hz, 4H); 4.98 (t, $J = 8.8$ Hz, 2H); 5.43 (dd, $J = 10.5$, 8.8 Hz, 2H); 5.55 (dd, $J = 10.5$, 8.8 Hz, 2H); 7.00 (d, $J = 8.7$ Hz, 4H); 7.38 (d, $J = 8.7$ Hz, 4H); 8.26 (d, $J = 8.1$ Hz, 2H); 8.73 (t, $J = 8.1$ Hz, 1H) ppm. ^{13}C NMR (CD_3NO_2) δ: 2.9; 15.0; 65.1; 67.7; 82.1; 116.4; 126.6; 129.4; 130.2; 130.9; 147.1; 147.6; 161.5; 171.9. MS (FAB) *m/e*: 582 (64); 563 (100). Analysis: Calc. for $C_{29}H_{30}N_4O_4B_2F_8Pd$ (778.59): C, 44.74; H, 3.88; N, 7.20%. Found: C, 44.39; H, 4.15; N, 6.86%.

3.6. Synthesis of [Pd($CNCH_2COOCH_3$)$_4$](BF_4)$_2$ (19)

[Pd(CH_3CN)$_4$](BF_4)$_2$ (119.0 mg, 2.68×10^{-4} mol) was dissolved in 5 ml of abs. acetonitrile and then treated with $CNCH_2CO_2Me$ (97.3 μl, 1.07×10^{-3} mol). Stirring for 30 min was followed by reducing the volume of the solvent to about 1 ml. Addition of ether induced precipitation of a brownish solid. The solvent was removed by decanting after centrifuging and then washed several times with ether. The product, 178.9 mg (98%) of **19**, was obtained after drying under vacuum. ^1H NMR (CD_3NO_2) δ: 3.89 (s, 3H); 5.04 (s, 2H) ppm. ^{13}C NMR (CD_3NO_2) δ: 49.8 [$J(^{14}N, ^{13}C) = 17.9$ Hz]; 116.4 [$J(^{14}N, ^{13}C) = 56.9$ Hz], ppm.

3.7. Synthesis of [Pd((S,S)-Ph-pybox)($CNCH_2COOCH_3$)](BF_4)$_2$ (15)

The same procedure was used as for **19** except that the appropriate stoichiometry was used. From **6** (46.7 mg, 6.76×10^{-5} mol) and methyl isocyanoacetate (6.2 μl, 6.79×10^{-5} mol) in 5 ml of acetonitrile one obtained 49.1 mg of **15** (97%) as a blue solid. IR (CsI) (cm^{-1}): 2277 (m); 1758 (s). ^1H NMR (CD_3NO_2) δ: 3.78 (s, 3H); 4.30 (s, 2H); 5.04 (t, $J = 8.8$ Hz, 2H); 5.51 (dd, $J = 10.5$, 8.8 Hz, 2H); 5.63 (dd, $J = 10.5$, 8.8 Hz, 2H); 7.4–7.5 (m, 10H); 8.37 (d, $J = 8.2$ Hz, 2H); 8.78 (t, $J = 8.2$ Hz, 1H) ppm. ^{13}C NMR (CD_3NO_2) δ: 46.9 [$J(^{14}N, ^{13}C) = 16.8$ Hz]; 54.8; 68.9; 82.3; 129.6; 130.4; 130.8; 131.3; 137.8; 146.4; 148.1; 163.5; 173.4. MS (FAB) *m/e*: 693 (31); 605 (69); 593 (19); 574 (13); 475 (80); 370 (14). Analysis: Calc. for $C_{27}H_{24}N_4O_4B_2F_8Pd$ (748.53): C, 43.32; H, 3.23; N, 7.48%. Found: C, 42.77; H, 3.54; N, 7.46%. A ^{13}C signal for $CNCH_2R$ was not observed.

3.8. Synthesis of [Pd((S,S)-Bz-pybox)($CNCH_2COOCH_3$)](BF_4)$_2$ (16)

The same procedure was used as for **15** except that the appropriate stoichiometry was used. Compound **7** (33.4 mg, 4.65×10^{-5} mol) and methyl isocyanoacetate (4.2 μl, 4.65×10^{-5} mol) in 5 ml of acetonitrile gave 30.0 mg (83%) of **16** as a blue solid. IR (CsI) (cm^{-1}): 2276 (m); 1759 (s). ^1H NMR (CD_3NO_2) δ: 3.08 (dd, $J = 14.0$, 7.0 Hz, 2H); 3.23 (dd, $J = 14.0$, 6.0 Hz, 2H); 3.79 (s, 3H); 4.8–4.9 (m, 2H); 4.86 (s, 2H); 5.05 (dd, $J = 9.7$, 5.7 Hz, 2H); 5.15 (t, $J = 9.5$ Hz, 2H); 7.2–7.5 (m, 10H); 8.19 (d, $J = 8.1$ Hz, 2H); 8.67 (t, $J = 8.1$ Hz, 1H) ppm. ^{13}C NMR (CD_3NO_2) δ: 40.7, 48.2 [$J(^{14}N, ^{13}C) = 17.4$ Hz]; 54.9; 65.8; 79.5; 128.9; 130.1; 130.4; 131.4; 135.9; 145.9; 148.2; 164.7; 173.4. MS (FAB) *m/e*: 621 (10); 602 (9); 503 (35); 398 (21). Analysis: Calc. for $C_{29}H_{28}N_4O_4B_2F_8Pd$ (776.58): C, 44.85; H, 3.63; N, 7.21%. Found: C, 44.71; H, 3.78; N, 7.11%. A ^{13}C signal for $CNCH_2R$ was not observed

3.9. Synthesis of $[Pd(CN^tBu)_4](BF_4)_2$ (17)

$[Pd(CH_3CN)_4][BF_4]_2$ (32.9 mg, 2.99×10^{-4} mol) in 5 ml of acetonitrile plus CN^tBu (142 μl, 1.26×10^{-3} mol) were stirred for 5 min. Reduction of the volume to about 1 ml was followed by addition of ether. Work-up as for **18** gave 176.0 mg of **17** (96%) as a white solid. IR (KBr) (cm^{-1}): 2268 (s). ^1H NMR (CD_3CN) δ: 1.60 (s, 36H) ppm. MS (FAB) *m/e*: 524 (35); 507 (14); 355 (5); 271 (9). Analysis: Calc. for $C_{20}H_{36}N_4B_2F_8Pd$ (612.55): C, 39.22; H, 5.92; N, 9.15%. Found: C, 39.42; H, 5.98; N, 9.25%.

3.10. Synthesis of [Pd(1,1'-bis(diphenylphosphino)ferrocene)$(CN^tBu)_2$]$(BF_4)_2$ (19)

The same procedure was used as for **17** except that the appropriate stoichiometry was used. $[Pd(CH_3CN)_2$-{(1,1'-bisdiphenylphosphino)ferrocene}$](BF_4)_2$ (50.1 mg, 5.47×10^{-5} mol) and CN^tBu (12.9 μl, 1.15×10^{-4} mol) in 3 ml of acetonitrile gave 51.5 mg of **19** (94%) as an orange solid. IR (KBr) (cm^{-1}): 2256 (s); 2247 (s). ^1H NMR (CD_3CN) δ: 1.15 (s, 18H); 4.38 (s, 4H); 4.70 (s, 4H); 7.5–7.8 (m, 20H) ppm. ^{31}P NMR (CD_3CN) δ: 30.06 ppm. MS (FAB) *m/e*: 913 (9); 762 (21); 743 (11); 679 (10); 660 (19). Analysis: Calc. for $C_{44}H_{46}N_2P_2B_2F_8FePd$ (1000.66); C, 52.81; H, 4.63; N, 2.80%. Found: C, 51.94; H, 4.80; N, 2.94%.

3.11. Synthesis of [Pd((S,S)-Ph-pybox)(η^3-C_3H_5)](OTf) (20)

$[Pd(\mu\text{-}Cl)(\eta^3\text{-}C_3H_5)]_2$ (69.4 mg, 1.90×10^{-4} mol) and **2** (140.2 mg, 3.80×10^{-4} mol) with AgOTf (107.4 mg, 4.18×10^{-4} mol) were suspended in 50 ml of acetone. After stirring for 1 h, the suspension was filtered through Celite and the solvent distilled. As a precautionary measure, the product was dissolved in CH_2Cl_2, filtered again and once again the solvent was distilled. Recrystallisation from CH_2Cl_2/ether gave 207.6 mg of **20** (82%) as colourless white needles; m.p. 163°C (decomp.); $[\alpha]_D^{22} = 108.5°$ ($c = 1.05$, $CHCl_3$). ^1H NMR ($CDCl_3$)δ: 2.48 (br, 1H); 2.65 (br, 1H); 3.34 (br, 1H); 3.73 (br, 1H); 4.56 (t, $J = 8.7$ Hz, 2H); 4.94 (quintet, $J = 9.4$ Hz, 1H); 5.12 (t, $J = 9.7$ Hz, 2H); 5.54 (dd, $J = 9.7$, 8.7 Hz, 2H); 7.2–7.4 (m, 10H); 8.25 (s, 3H) ppm. ^{13}C NMR ($CDCl_3$)δ: 61.2; 62.1; 70.3; 76.9; 114.2; 127.1; 128.2; 128.5; 128.9; 139.1; 140.2; 145.5; 165.4. MS (FAB) *m/e*: 666 (< 1); 624 (7); 516 (100); 475 (42); 370 (4). Analysis: Calc. for $C_{27}H_{24}N_3O_5F_3SPd$ (665.98): C, 48.69; H, 3.63; N, 6.31%. Found: C, 47.90; H, 3.68; N, 6.10%.

3.12. Synthesis of [Pd((S,S)-Bz-pybox)(4-picoline)]-$[BF_4]_2$ (21a)

4-Picoline (2.9 mg, 3.07×10^{-5} mol) was dissolved in 2 ml of methanol, then treated with **7** (22.1 mg, 3.07×10^{-5} mol) and stirred for 20 min. Concentration to ca. 1 ml was followed by addition of ether. The yellow solid which precipitated was collected via filtration, washed with ether and dried: 21.3 mg (90%). ^1H NMR (CD_3OD)δ: 2.48 (dd, $J = 14.0$, 5.4 Hz, 2H); 2.61 (s, 3H); 2.63 (dd, $J = 14.0$, 7.5 Hz, 2H); 4.7–4.8 (m, 2H); 4.97 (dd, $J = 9.4$, 5.7 Hz, 2H); 5.13 (t, $J = 9.4$ Hz, 2H); 7.1–7.3 (m, 10H); 7.68 (d, $J = 6.5$ Hz, 2H); 8.26 (d, $J = 8.0$ Hz, 2H); 8.67 (t, $J = 8.0$ Hz, 1H); 8.76 (d, $J = 6.5$ Hz, 2H) ppm. ^{13}C NMR (CD_3OD)δ: 22.1; 41.1; 64.6; 79.7; 129.3; 130.0; 130.6; 130.9; 131.2; 136.4; 145.2; 147.5; 153.0; 157.0; 173.1. Analysis: Calc. for $C_{31}H_{30}N_4O_2B_2F_8Pd$ (770.62): C, 48.32; H, 3.92; N, 7.27%. Found: C, 48.02; H, 4.14; N, 7.14%.

3.13. Synthesis of [Pd((S,S)-Bz-pybox)(2,6-lutidine)]$[BF_4]_2$ (21b)

The preparation was the same as for **21a**. 2,6-Lutidine (4.4 mg, 4.11×10^{-5} mol) and **7** (29.5 mg, 4.11×10^{-5} mol) gave 30.0 mg (93%) of **21b** as a yellow powder. ^1H NMR (CD_3NO_2)δ: 2.28 (dd, $J = 13.7$, 4.0 Hz, 2H); 2.79 (dd, $J = 13.7$, 10.1 Hz, 2H); 3.46 (s, 6H); 4.5–4.6 (m, 2H); 4.90 (dd, $J = 9.4$, 7.2 Hz, 2H); 5.07 (t, $J = 9.4$ Hz, 2H); 6.9–7.0 (m, 4H); 7.2–7.3 (m, 6H); 7.62 (d, $J = 7.8$ Hz, 2H); 8.08 (t, $J = 7.8$ Hz, 1H);8.22 (d, $J = 8.0$ Hz, 2H); 8.70 (t, $J = 8.0$ Hz, 1H) ppm. ^{13}C NMR (CD_3NO_2)δ: 26.5; 40.2; 65.2; 79.2; 126.8; 128.8; 129.8; 130.2; 130.3; 135.7; 143.5; 146.3; 147.3; 161.9; 173.0. Analysis: Calc. for $C_{32}H_{32}N_4O_2B_2F_8Pd$ (784.65): C, 48.98; H, 4.11; N, 7.14%. Found: C, 48.59; H, 4.59; N, 7.08%.

3.14. Synthesis of [Pd((S,S)-Bz-pybox)(P-toluidine)]-$[BF_4]_2$ (21c)

The preparation was the same as for **21a**. P-Toluidine (3.7 mg, 3.45×10^{-5} mol) and **7** (24.8 mg, 3.45×10^{-5} mol) gave 23.6 mg (87%) of **21c** as a yellow solid. ^1H NMR (CD_3OD)δ: 2.29 (s, 3H); 2.65 (dd, $J = 14.3$, 5.2 Hz, 2H); 2.80 (dd, $J = 14.3$, 7.2 Hz, 2H); 4.3–4.5 (m, 2H); 4.90 (dd, $J = 9.2$, 4.3 Hz, 2H); 4.99 (t, $J = 9.2$ Hz, 2H); 7.2–7.4 (m, 12H); 7.59 (d, $J = 8.4$ Hz, 2H); 8.12 (d, $J = 8.1$ Hz, 2H); 8.59 (t, $J = 8.1$ Hz, 1H) ppm. ^{13}C NMR (CD_3OD)δ: 21.7; 40.5; 64.9; 78.8; 125.2; 129.4; 129.7; 130.9; 131.6; 132.7; 136.8; 139.5; 140.1; 146.9; 147.2; 173.1 ppm. Analysis: Calc. for $C_{32}H_{32}N_4O_2$-B_2F_8Pd (784.65): C, 48.98; H, 4.11; N, 7.14%. Found: C, 48.89; H, 4.35; N, 6.88%.

3.15. Synthesis of [Pd((S,S)-Bz-pybox)(H_2NCH_2-$CH(OCH_3)_2$)]$[BF_4]_2$ (21d)

The preparation was the same as for **21a**. Aminoacetaldehyde dimethylacetal (5.4 mg, 5.14×10^{-5} mol) and **7** (36.9 mg, 5.14×10^{-5} mol) gave 31.8 mg (79%) of **21d** as a yellow solid. ^1H NMR (CD_3OD)δ: 2.94 (d,

$J = 4.0$ Hz, 2H); 3.08 (dd, $J = 14.0$, 6.9 Hz, 2H); 3.22 (dd, $J = 14.0$, 5.9 Hz, 2H); 3.50 (s, 6H); 4.61 (t, $J = 4.0$ Hz, 1H); 4.8–4.9 (m, 2H); 4.99 (dd, $J = 9.2$, 4.6 Hz, 2H); 5.05 (t, $J = 9.2$ Hz, 2H); 7.3–7.6 (m, 10H); 8.13 (d, $J = 8.0$ Hz, 2H); 8.58 (t, $J = 8.0$ Hz, 1H) ppm. ^{13}C NMR (CD_3OD)δ: 41.1; 56.9; 65.6; 67.6; 79.2; 104.3; 129.6; 129.8; 131.0; 131.8; 137.0; 143.4; 147.0; 173.2. Analysis: Calc. for $C_{29}H_{34}N_4O_4B_2F_8Pd$ (782.63): C, 44.51; H, 4.38; N, 7.16%. Found: C, 45.05; H, 4.42; N, 6.91%.

3.16. Synthesis of [Pd((S,S)-Bz-pybox)($H_2NCH_2CH_2OH$)][BF_4]$_2$ (21e)

The preparation was the same as for **21a**. Ethanolamine (4.3 mg, 7.04×10^{-5} mol) and **7** (50.6 mg, 7.04×10^{-5} mol) gave 43.2 mg (83%) of **21e** as a yellow solid. ^{1}H NMR (CD_3OD)δ: 2.92 (t, $J = 4.7$ Hz, 2H); 3.08 (dd, $J = 13.9$, 6.9 Hz, 2H); 3.24 (dd, $J = 13.9$, 5.9 Hz, 2H); 3.42 (t, $J = 4.7$ Hz, 2H); 3.8–3.9 (m, 2H); 4.9–5.1 (m, 4H); 7.3–7.6 (m, 10H); 8.16 (d, $J = 8.0$ Hz, 2H); 8.60 (t, $J = 8.0$ Hz, 1H) ppm. ^{13}C NMR (CD_3NO_2)δ: 40.8; 49.5; 61.4; 65.0; 79.0; 129.1; 129.5; 130.5; 131.3; 136.3; 145.9; 146.9; 172.5. Analysis: Calc. for $C_{27}H_{30}N_4O_3B_2F_8Pd$ (738.57): C, 43.91; H, 4.09; N, 7.59%. Found: C, 44.49; H, 4.45; N, 7.65%.

3.17. Synthesis of [Pd((S,S)-Bz-pybox)($H_2N(CH_2)_5CH_3$)][BF_4]$_2$ (21f)

The preparation was the same as for **21a**. Hexylamine (3.8 mg, 3.60×10^{-5} mol) and **7** (25.9 mg, 3.60×10^{-5} mol) gave 23.8 mg (85%) of **21f** as a yellow solid. ^{1}H NMR (CD_3NO_2)δ: 0.85 (t, $J = 6.5$ Hz, 3H); 1.2–1.4 (m, 6H); 1.5–1.7 (m, 2H); 2.6–2.8 (m, 2H); 2.9–8.1 (m + br, 5H); 4.7–4.9 (m, 2H); 5.05 (dd, $J = 9.1$, 4.6 Hz, 2H); 5.14 (t, $J = 9.1$ Hz, 2H); 7.3–7.5 (m, 10H); 8.15 (d, $J = 8.0$ Hz, 2H); 8.64 (t, $J = 8.0$ Hz, 1H) ppm. ^{13}C NMR (CD_3NO_2)δ: 14.2; 23.4; 27.2; 32.2; 32.3; 41.2; 48.2; 65.1; 79.3; 129.3; 129.6; 130.7; 131.1; 136.4; 145.9; 146.9; 172.6. Analysis: Calc. for $C_{31}H_{38}N_4O_2B_2F_8Pd$ (778.68): C, 47.82; H, 4.92; N, 7.20%. Found: C, 46.65; H, 4.47; N, 7.43%.

3.18. Synthesis of [Pd((S,S)-Bz-pybox)(PPh_3)][BF_4]$_2$ (21g)

The preparation was the same as for **21a**. Triphenylphosphine (33.1 mg, 1.26×10^{-4} mol) in 3 ml of CH_2Cl_2 at −78°C and a solution of **7** (90.7 mg, 1.26×10^{-4} mol) in 2 ml of acetonitrile were warmed slowly to room temperature. The suspension which resulted was taken to dryness. Recrystallisation from acetonitrile/ether gave 90.1 mg (76%) of **21g**. ^{1}H NMR (CD_3NO_2)δ: 2.1–2.3 (m, 4H); 3.5–3.7 (m, 2H); 4.7–4.8 (m, 2H); 6.7–6.8 (m, 4H); 7.1–7.2 (m, 6H); 7.6–7.9 (m, 9H); 8.1–8.3 (m, 8H); 8.64 (t, $J = 7.9$ Hz, 1H), ppm. ^{13}C NMR (CD_3NO_2)δ: 39.5, 63.9, 77.5, 127.5 [$^1J(^{31}P, ^{13}C) = 55.0$ Hz]; 128.6, 129.5 [$^4J(^{31}P, ^{13}C) = 1.9$ Hz]; 130.0, 130.6, 131.5 [$^3J(^{31}P, ^{13}C) = 11.9$ Hz]; 135.1, 135.3 [$^4J(^{31}P, ^{13}C) = 2.8$ Hz]; 136.4 [$^2J(^{31}P, ^{13}C) = 11.7$ Hz]; 144.6 [$^5J(^{31}P, ^{13}C) = 1.9$ Hz]; 147.5, 173.8 ppm. ^{31}P NMR (CD_3NO_2)δ: 21.94 ppm. MS (FAB) *m/e*: 919 (10); 766 (24); 503 (55) (100). Analysis: Calc. for $C_{43}H_{38}N_3O_2PB_2F_8Pd$ (939.78): C, 54.96; H, 4.08; N, 4.47%. Found: C, 54.89; H, 4.24; N, 4.57%.

3.19. Synthesis of [Pd((S,S)-Bz-pybox)(N_3)][BF_4] (21h)

The preparation was the same as for **21a**. Sodium azide (3.2 mg, 4.97×10^{-5} mol) was dissolved in 2 ml of methanol and then treated with a solution of **7** (35.7 mg, 4.97×10^{-5} mol) in 5 ml of methanol. Stirring for 30 min at room temperature was followed by removal of the solvent under vacuum. The residue was taken up in CH_2Cl_2 and filtered through Celite. Addition of ether gave 30.4 mg (97%) of **21h** as a yellow solid. ^{1}H NMR (CD_3NO_2)δ: 3.06 (dd, $J = 13.9$, 8.4 Hz, 2H); 3.37 (dd, $J = 13.9$, 3.8 Hz, 2H); 4.7–4.8 (m, 2H); 4.97 (dd, $J = 9.5$, 6.2 Hz, 2H); 5.07 (t, $J = 9.6$ Hz, 2H); 7.2–7.5 (m, 10H); 8.04 (d, $J = 8.0$ Hz, 2H); 8.50 (t, $J = 8.0$ Hz, 1H) ppm. ^{13}C NMR (CD_3NO_2)δ: 39.7; 63.9; 78.3; 128.6; 128.9; 130.1; 131.2; 136.3; 145.5; 145.6; 171.6. Analysis: Calc. for $C_{25}H_{23}N_6O_2BF_4Pd$ (632.71): C, 47.46; H, 3.66; N, 13.28%. Found: C, 47.41; H, 3.88; N, 13.10%.

3.20. Synthesis of [Pd((S,S)-Ph-pybox)(OCOH)][BF_4]

The preparation was the same as for **21a**. Sodium formate (2.6 mg, 3.82×10^{-5} mol) was dissolved in 2 ml of methanol and then treated with a solution of **2** (26.4 mg, 3.82×10^{-5} mol) in 3 ml of methanol. After stirring for 30 min at room temperature, the solvent was distilled. The residue was taken up in CH_2Cl_2 and then filtered through Celite. Addition of ether induced precipitation of the product which, after several washings with ether, could be collected and dried to afford 18.1 mg (78%) of product. ^{1}H NMR (CD_3NO_2)δ: 5.00 (dd, $J = 9.0$, 8.0 Hz, 2H); 5.34 (dd, $J = 10.5$, 8.0 Hz, 2H); 5.50 (dd, $J = 10.5$, 9.0 Hz, 2H); 6.61 (s, 1H); 7.3–7.5 (m, 10H); 8.20 (d, $J = 8.1$ Hz, 2H); 8.63 (t, $J = 8.1$ Hz, 1H) ppm. ^{13}C NMR (CD_3NO_2)δ: 67.8; 81.9; 128.9; 129.3; 130.2; 130.4; 138.7; 145.8; 146.5; 168.6; 171.1. Analysis: Calc. for $C_{24}H_{20}N_3O_4BF_4Pd$ (607.66): C, 47.44, H, 3.32, N, 6.92%. Found: C, 46.99; H, 3.39; N, 6.85%.

3.21. Synthesis of [Pd((S,S)-Bz-pybox)(OCOH)][BF_4] (21i)

The preparation was the same as for **21a**. From sodium formate (6.9 mg, 1.01×10^{-4} mol) and **7** (72.9

mg, 1.01×10^{-4} mol) was obtained 18.1 mg (78%) of **21i** as a yellow solid. ^{1}H NMR (CD_3NO_2)δ: 2.95 (dd, J = 13.9, 8.0 Hz, 2H); 3.15 (dd, J = 13.9, 3.7 Hz, 2H); 4.6–4.8 (m, 2H); 4.84 (dd, J = 9.2, 7.0 Hz, 2H); 4.98 (t, J = 9.6 Hz, 2H); 7.2–7.5 (m, 10H); 7.74 (s, 1H); 7.93 (d, J = 8.1 Hz, 2H); 8.43 (t, J = 8.1 Hz, 1H) ppm. ^{13}C NMR (CD_3NO_2)δ: 39.6; 65.3; 78.5; 128.6; 128.9; 130.1; 131.1; 136.5; 145.9; 146.4; 169.9; 171.0 ppm.

3.22. Synthesis of [Pd((S,S)-Ph-pybox)Cl] (OTf)

$Pd(CH_3CN)_2Cl_2$ (219.1 mg, 8.45×10^{-4} mol) was dissolved in 10 ml of CH_3CN and then treated with **2** (312.0 mg, 8.45×10^{-4} mol). After several minutes of stirring, AgOTf (217.0 mg, 8.45×10^{-4} mol) was added. After an additional 10 min, the AgCl was filtered over Celite and the solvent distilled under vacuum. Redissolution in CH_2Cl_2 was followed by another filtration through Celite. Treatment with hexane gave an orange–yellow solid which was recrystallised from CH_3CN/CH_2Cl_2/ether to afford the analogue of **21j**, 414.3 mg (74%), as orange crystals; m.p. 169°C (decomp.). IR (CsI) (cm^{-1}): 334 (w). ^{1}H NMR (CD_3CN)δ: 4.92 (dd, J = 4.9, 2.2 Hz, 2H); 5.33 (dd, J = 10.4, 4.9 Hz, 2H); 5.36 (dd, J = 10.4, 2.2 Hz, 2H); 7.39 (s, 10H); 8.18 (d, J = 8.1 Hz, 2H); 8.56 (t, J = 8.1 Hz, 1H) ppm. ^{13}C NMR (CD_3CN)δ: 66.9; 81.9; 128.7; 129.3; 129.7; 129.9; 139.1; 145.2; 145.8; 171.7 ppm. MS (FAB) m/e: 512 (100); 475 (43); 370 (7). Analysis: Calc. for $C_{24}H_{19}N_3O_5F_3SClPd$ (660.36): C, 43.65; H, 2.90; N, 6.36%. Found: C, 43.82; H, 3.01; N, 6.21%.

3.23. Synthesis of [Pd((S,S)-Bz-pybox)Cl](OTf)

The method of **21j** was used for this complex. $Pd(CH_3CN)_2Cl_2$ (7.9 mg, 3.39×10^{-4} mol), **3** (134.7 mg, 3.39×10^{-4} mol) and AgOTf (87.1 mg, 3.39×10^{-4} mol) gave the complex **21j**, 221.7 mg (95%); m.p. 129°C (decomp.). IR (CsI) (cm^{-1}): 314 m). ^{1}H NMR ($CDCl_3$)δ: 3.06 (dd, J = 13.7, 8.8 Hz, 2H); 3.51 (dd, J = 13.7, 3.2 Hz, 2H); 4.6–4.7 (m, 2H); 4.80 (dd, J = 9.1, 6.6 Hz, 2H); 4.91 (t, J = 9.5 Hz, 2H); 7.2–7.4 (m, 10H); 7.97 (d, J = 8.0 Hz, 2H); 8.46 (t, J = 8.0 Hz, 1H) ppm. ^{13}C NMR ($CDCl_3$)δ: 38.6; 63.5; 76.6; 127.2; 127.7; 128.8; 129.3; 134.5; 143.8; 144.1; 169.7 ppm. MS (FAB) m/e: 540 (100); 503 (36) ppm. Analysis: Calc. for $C_{26}H_{23}N_3O_5F_3SClPd$ (688.41): C, 45.36; H, 3.37; N, 6.10%. Found: C, 45.14; H, 3.65; N, 6.03%.

3.24. Synthesis of [Pd((S,S)-Bz-pybox)(NCCH=CH$_2$)][BF$_4$]$_2$ (21k)

Complex **7** (54.6 mg, 7.60×10^{-5} mol) in 5 ml of Acrylonitrile was stirred for 30 min at room temperature. Excess acrylonitrile was removed (trapped with a cold receiver) and the resulting oil dissolved in nitromethane. Addition of ether afforded a yellow solid which after several washings with ether was collected as the product; 55.4 mg (> 99%). ^{1}H NMR (CD_3NO_2, −10°C)δ: 3.04 (dd, J = 14.1, 6.9 Hz, 2H); 3.14 (dd, J = 14.1, 6.2 Hz, 2H); 4.7–4.9 (m, 2H); 5.02 (dd, J = 9.4, 5.5 Hz, 2H); 5.11 (t, J = 9.4 Hz, 2H); 6.14 (dd, J = 17.9, 12.0 Hz, 1H); 6.61 (d, J = 12.0 Hz, 1H); 6.72 (d, J = 17.9 Hz, 1H); 7.2–7.5 (m, 10H); 8.12 (d, J = 8.1 Hz, 2H); 8.61 (t, J = 8.1 Hz, 1H) ppm. ^{13}C NMR (CD_3NO_2)δ: 40.6; 65.1; 79.4; 106.2; 124.6; 128.9; 130.0; 130.5; 131.2; 136.1; 139.7; 146.7; 147.7; 172.3. Analysis: Calc. for $C_{28}H_{26}N_4O_2B_2F_8Pd$ (730.52): C, 46.03; H, 3.59; N, 7.67%. Found: C, 45.75; H, 3.88; N, 7.54%.

Acknowledgements

P.S.P. thanks the Swiss National Science Foundation as well as the ETH for support, and the Johnson-Matthey Research Foundation, Reading, England for the loan of precious metals. We also thank Dr. Renzo Salzmann for experimental assistance.

Supplementary material available

Coefficients of the anisotropic temperature factors for **6** (Tables S1–S3, 1 p. each); positional parameters and isotropic equivlaent displacement parameters for **6**, calculated hydrogen positions (Tables S4 and S5, 1 p. each); extended list of bond lengths and bond angles for **6** (Table S6, 6 pp.); anisotropic displacement parameters for **21g** (Table S7, 2 pages); calculated positional parameters for the hydrogen atoms in **21g** (Table S8, 2 pp.); extended list of bond lengths, bond angles and torsion angles for **21g** (Table S9, 8 pp.); observed and calculated structure factors for **6** and for **21g** (27 and 22 pp., respectively).

References

[1] (a) H.M. Colquhoun, J. Holton, J.D.T. Thompson and M.V. Twigg (eds.), *New Pathways for Organic Synthesis*, Plenum, New York, 1984; (b) B.M. Trost, *Chemtracts-Org. Chem., 1* (1988) 415; (c) B.M. Trost, *Tetrahedron, 33* (1977) 2625; (d) B.M. Trost, *Acc. Chem. Res., 13* (1980) 385; (e) A.J. Pearson, *Metallo-Organic Chemistry*, John Wiley & Sons, New York, 1985; (f) I. Stary and I.P. Kocovsky, *J. Am. Chem. Soc., 111* (1989) 4981.

[2] R. Noyori and M. Kiramura, in R. Sheffold (ed.), *Modern Synthetic Methods*, Springer-Verlag, Berlin, 1989, p. 119; J.M. Brown, *Chem. Br.*, (1989) 276; W.S. Knowles, *Acc. Chem. Res., 16* (1983) 106. See also *Chem. Rev., 92* (1992) 5.

[3] R. Nesper, P.S. Pregosin, K. Püntener and M. Wörle, *Helv. Chim. Acta, 76* (1993) 2239.

[4] (a) T. Hayashi, M. Sawamura and Y. Ito, *Tetrahedron, 48* (1992) 1999; (b) Y. Ito, M. Sawamura, E. Shirakawa, K. Hayashizaki and T. Hayashi, *Tetrahedron Lett., 29* (1988) 235; (c) M. Sawamura, Y. Ito and T. Hayashi, *Tetrahedron Lett., 30* (1989) 2247; (d) T. Hayashi, M. Sawamura and Y. Ito, *Tetrahedron Lett., 29* (1989) 6321; (e) Y. Ito, M. Sawamura, E. Sirkawa, Hayashi, K. Zaki and T. Hayashi, *Tetrahedron Lett., 44* (1988) 5253; (f) Y. Ito, M. Sawamura, M. Kabayashi and T. Hayashi, *Tetrahedron Lett., 29* (1988) 239; (g) Y. Ito, M. Sawamura and T. Hayashi, *Tetrahedron Lett.*, 28 (1987) 6215; (h) Y. Ito, M. Sawamura and T. Hayashi, *J. Chem. Soc., Chem. Commun.*, (1986) 1090; (i) Y. Ito, M. Sawamura and T. Hayashi, *J. Am. Chem. Soc., 108* (1986) 6405.

[5] (a) A. Togni and S.D. Pastor, *J. Org. Chem., 55* (1990) 1649; (b) S.D. Pastor and A. Togni, *Helv. Chim. Acta, 74* (1991) 905; (c) A. Togni, S.D. Pastor and G. Rihs, *J. Organomet. Chem., 38* (1990) C21; (d) A. Togni and S.D. Pastor, *Helv. Chim. Acta, 72* (1989) 1038; (e) A. Togni and S.D. Pastor, *Tetrahedron Lett., 30* (1989) 1071; (f) A. Togni and R. Häusel, *Synlett.*, (1990) 633.

[6] H. Nishiyama, M. Kondo, T. Nakamura and K. Itsch, *Organometallics, 10* (1991) 500.

[7] B.B. Wayland and R.F. Schramm, *Chem. Commun.*, (1968) 898; B.B. Wayland and R.F. Schramm, *Inorg. Chem., 8* (1969) 971; R.R. Thomas, A. Sen., W. Beck and R. Leidl, *Inorg. Synth., 28* (1990) 63.

[8] B.A. Markies, P. Wijkens, J. Boersma, H. Kooijman, A.L. Spek and G. van Koten, *Organometallics, 13* (1994) 3244; P. Castan, F. Dahan, S. Wimmer and F. Wimmer, *J. Chem. Soc., Dalton Trans.*, (1990) 2679.

[9] M. Sommovigo, M. Pasquali, P. Leoni, P. Sabatino and D. Braga, *J. Organomet. Chem., 418* (1991) 119.

[10] T. Appleton, H.C. Clark and L.E. Manzer, *Coord. Chem. Rev., 10* (1973) 335; H. Motschi, P.S. Pregosin and L.M. Venanzi, *Helv. Chim. Acta, 62* (1979) 667; H. Motschi and P.S. Pregosin, *Inorg. Chim. Acta, 40* (1980) 141; H. Motschi, C. Nussbaumer, F. Bachechi, C. Mura and P.S. Pregosin, *Inorg. Chim. Acta, 63* (1980) 2071.

[11] M. Oshima, A. Yamamoto and F. Ozawa, *Organometallics, 10* (1991) 1221.

[12] D. Carmona, S. Chalopka, J. Jans, R. Thouvenot and L.M. Venanzi, *J. Organomet. Chem., 275* (1984) 303; G. Bracher, B. Kellenberger, L.M. Venanzi, F. Bachechi and L. Zambonelli, *Helv. Chim. Acta, 71* (1988) 1442.

[13] A. Albinati, C. Arz and P.S. Pregosin, *Inorg. Chem., 26* (1987) 508.

[14] G. Ferguson, R. McCrindle, A.J. McAlees and M. Parvez, *Acta Crystallogr., B38* (1982) 2679.

[15] E. Binamira-Soriaga, M. Lundeen and K. Seff, *J. Cryst. Mol. Struct., 9* (1979) 71.

[16] W. Zhang, C. Bensimon and R.J. Crutchley, *Inorg. Chem., 32* (1993) 5808.

[17] (a) S. Wimmer, P. Castan, F. Wimmer and N.P. Johnson, *J. Chem. Soc., Dalton Trans.*, (1989) 403; (c) G. Lopez, J. Ruiz, G. Garcia, C. Vicente, J. Casabo, E. Molins and C. Miravitlles, *Inorg. Chem., 30* (1991) 2605; G. Lopez, J. Ruiz, G. Garcia, C. Vicente, J.M. Marti and M.D. Santana, *J. Organomet. Chem., 393* (1990) C53.

[18] MOLEN: *Molecular Structure Solution Procedure*, Enraf-Nonius, Delft, The Netherlands, 1990.

[19] *International Tables for X-ray Crystallography*, Kynoch Press, Birmingham, England, 1974, Vol. IV.

[20] W.C. Hamilton, *Acta Crystallogr., 13* (1965) 502.